Period adding structure in a 2D discontinuous model of economic growth

Fabio Tramontana[a1], **Iryna Sushko**[b], **Viktor Avrutin**[c]

[a] Department of Economics and Management, University of Pavia, Italy
[b] Institute of Mathematics, National Academy of Sciences of Ukraine, and Kyiv School of Economics
[c] University of Urbino Carlo Bo, Urbino, Italy, and IST, University of Stuttgart, Stuttgart, Germany

Abstract.

We study the dynamics of a growth model formulated in the tradition of Kaldor and Pasinetti where the accumulation of the ratio capital/workers is regulated by a two-dimensional discontinuous map with triangular structure. We determine analytically the border collision bifurcation boundaries of periodicity regions related to attracting cycles, showing that in a two-dimensional parameter plane these regions are organized in the period adding structure. We show that the cascade of flip bifurcations in the base one-dimensional map corresponds for the two-dimensional map to a sequence of pitchfork and flip bifurcations for cycles of even and odd periods, respectively.

Keywords: Discontinuous maps, Two-dimensional piecewise smooth maps, Border collision bifurcations, Growth models.

1 Introduction

An important limitation of neoclassical models of economic growth consists in exclusively predicting for the long run a monotonic convergence to a steady state for both output and capital per capita. A lot of efforts have been made by economists to conceive the possibility of endogenous growth cycles. If we only focus on the so-called Solow-Swan growth model, it has been proved, for instance, that complicated growth paths may arise by considering two sectors instead of one, combined with certain levels of discounting (see [1],[2]). Other researchers have introduced economically founded nonlinearities into the models in order to make unstable the steady state or even increase the number of stationary states, with the possibility of complicated dynamics. A pioneer in this strand of research is Richard Day, who in a pair of seminal papers [3],[4] improved the Solow model introducing some nonlinearities leading to irregular growth cycles. One of these possibilities consists in replacing the unrealistic hypothesis of exponential growth of the labor force with a more realistic bounded growth such as the logistic one. This alternative formalization of the labor force growth rate has been successfully implemented into the classical Ramsey growth model [5]-[10], the Solow-Swan framework [11] and the Kaldor-Pasinetti model with differential savings [12].

Endogenous fluctuations of the growth path can also be generated by the introduction of discontinuities in an otherwise classical framework. From a mathematical point of view a discontinuity, like a nonlinearity, may cause the emergence of complex dynamics (cycles and chaos), however routes to such dynamics are quite different. To our knowledge only Böhm and Kaas [13] and Tramontana et al. [14] give examples of investigations of the role of a discontinuity in a classical growth model[2]. They move from a Kaldor-Pasinetti model with differential savings and introduce a discontinuity through a Leontief production function, showing that growth cycles are a typical outcome under these assumptions.

Recently, in [17] a growth model is built which combines the nonlinearity of the logistic growth of the labor force with the discontinuity arising from the assumption of Leontief technology (as in [13] and [14]).

---

[2]In fact we should also mention the growth model studied by Matsuyama [15] and Gardini et al. [16] where combining Solow and Romer models a piecewise smooth map is obtained. However, the map is continuous, and this leads to dynamics quite different from those occurring in a discontinuous one.

The authors explain the economic meaning of these assumptions and show some numerical simulations with interesting dynamic outcomes.

The aim of the present paper is to investigate the bifurcations occurring in the model proposed in [17], which is described by a two-dimensional (2D henceforth in short) discontinuous triangular map base of which is the well known logistic map. We show that quite complicated growth paths may emerge and some of the observed phenomena are qualitatively different from those arising in models with nonlinearities and discontinuities taken separately. In particular, bistability is proved to occur in the present 2D map. Moreover, we show that the periodicity regions related to stable cycles are organized in the period adding structure. Note that such a structure is characteristic for a class of one-dimensional (1D for short) discontinuous piecewise monotone maps (see, among others, [18], [19], [20], [14]). It has been shown that the period adding structure can be observed also in 1D maps with two discontinuities [21], and in continuous 1D maps with two border points [22]. A first example of the period adding structure in 2D discontinuous maps is provided in [23]. In the present paper we explain how to obtain analytically the equations of the border collision bifurcation[3] (BCB for short) boundaries of the periodicity regions in the parameter space.

The paper is organized as follows. In Sec. 2 we introduce the economic assumptions that permit to obtain a 2D discontinuous map governing the dynamics of the capital accumulation. Some preliminary results are presented in Sec. 3. Different bifurcation scenarios originating by the map are studied in the subsequent three sections. In particular, in Sec. 4 we describe the asymptotic dynamics occurring in a 1D piecewise linear map with one discontinuity, which is a restriction of the 2D map to an invariant straight line (layer) associated with the fixed point of the base map. A first period doubling bifurcation of this fixed point leads to two cyclic layers (associated with the 2-cycle of the logistic map) on which the restriction of the 2D map is a 1D piecewise linear map with at most three discontinuity points. The asymptotic dynamics of this map is studied in Sec.5. These 1D maps allow us to explain the existence of a period adding structure in the parameter space of the 2D map, and to determine analytically the equations of the border collision bifurcations boundaries of the periodicity regions presented in Appendix. In Sec.6 we prove the occurrence of bistability associated with flip bifurcations in the base map, which for the 2D map are pitchfork bifurcations (leading thus to bistability) for the cycles of even periods or flip bifurcations for the cycles of odd periods. In Sec.7 we propose some final observations.

2   The model

We consider a classic discrete time one sector Solow-Swan growth model enriched by the following additional assumptions:

- two groups of agents, workers and shareholders (see [24]-[26]) are characterized by constant but different saving propensities, usually denoted as s_w and s_r in the cited literature, and here denoted in a concise form as w and r, with $0 \leq w \leq r \leq 1$;

- technology is characterized by a Leontief production function (see [13]):

$$f(k) = \min(ak, b) + c \tag{1}$$

  where k denotes capital per worker, and a, b, c are positive technical parameters;

- a logistic labor force growth rate (n).

The usual way of determining the wage rate W is:

$$W(k) = f(k) - kf'(k), \tag{2}$$

where the marginal product $f'(k)$ is what shareholders gather while $kf'(k)$ is the capital income per worker.

Considering a one-period production lag and a capital depreciation rate $0 < \delta \leq 1$ we get the following equation that regulates the growth path of the capital accumulation:

$$k_{t+1} = \frac{1}{1 + n_t} \left[(1 - \delta) k_t + wW(k_t) + rk_t f'(k_t) \right]. \tag{3}$$

---

[3]Recall that in discontinuous maps the BCB of a cycle occurs when one of its periodic points collides with the border of the existence region of the cycle, causing its appearance or disappearance.

Substituting the wage rate equation (2), using the Leontief production function (1) and the assumption of logistic capital force growth rate, we finally obtain the following 2D discontinuous map:

$$k' = \begin{cases} \frac{1}{1+n}\left[(1-\delta+s_r a)\,k + s_w c\right] & \text{if} \quad k \le \frac{b}{a} \\ \frac{1}{1+n}\left[(1-\delta+s_r a)\,k + s_w c\right] & \text{if} \quad k > \frac{b}{a} \end{cases}, \tag{4}$$
$$n' = \mu n(1-n),$$

where μ is the parameter regulating the dynamic of the logistic function.

Let us rewrite the map (4) it in a more convenient form. We set the state variables as a vector $(x,y) = (k,n) \in \mathbb{R}_+^2$ and consider the family of 2D discontinuous piecewise smooth maps $T : \mathbb{R}_+^2 \to \mathbb{R}_+^2$ defined as

$$T : \begin{pmatrix} x \\ y \end{pmatrix} \mapsto \begin{pmatrix} G(x,y) \\ f(y) \end{pmatrix}, \tag{5}$$

where

$$G(x,y) = \begin{cases} G_L(x,y) = \dfrac{(1-\delta+ra)\,x + wc}{1+y} & \text{if} \quad x \le \dfrac{b}{a} \\ G_R(x,y) = \dfrac{(1-\delta)\,x + w(b+c)}{1+y} & \text{if} \quad x > \dfrac{b}{a} \end{cases}, \tag{6}$$
$$f(y) = \mu y(1-y),$$

and we recall that the parameters introduced above, that is, a, b, c, δ, r, w and μ, are considered satisfying the following restrictions:

$$a,b,c > 0, \quad 0 < \delta \le 1, \quad 0 < w < r < 1, \quad 1 < \mu < 4. \tag{7}$$

3   Preliminaries

First we note that map T belongs to the class of *triangular* maps[4] given that the function which governs the dynamics of the variable y does not depend on the variable x. In fact, the so-called base map $y \mapsto f(y)$ is the well-known *logistic map* whose dynamic properties can be used to describe the dynamics of T. As already remarked, one more peculiarity of map T is that it is a *discontinuous piecewise smooth* map. The line

$$C_{-1} = \left\{ (x,y) \in \mathbb{R}_+^2 : \; x = b/a \right\},$$

on which map T is discontinuous separates the phase plane of T in two partitions, denoted by D_L and D_R, in which smooth maps T_L and T_R, respectively, are defined:

$$T_L : \begin{pmatrix} x \\ y \end{pmatrix} \mapsto \begin{pmatrix} G_L(x,y) \\ f(y) \end{pmatrix}, \; (x,y) \in D_L = \left\{ (x,y) \in \mathbb{R}_+^2 : \; x \le b/a \right\},$$

$$T_R : \begin{pmatrix} x \\ y \end{pmatrix} \mapsto \begin{pmatrix} G_R(x,y) \\ f(y) \end{pmatrix}, \; (x,y) \in D_R = \left\{ (x,y) \in \mathbb{R}_+^2 : \; x > b/a \right\}.$$

Following [35] and [36], the discontinuity line C_{-1} as well as its images $C^L = T_L(C_{-1})$ and $C^R = T_R(C_{-1})$ are called *critical lines*. The images and preimages of C_{-1} play an important role in the description of the dynamics of map T, similar to the role of critical lines for smooth noninvertible 2D maps and the role of critical (folding) points for smooth noninvertible 1D maps.

It is easy to see that map T can have at most *two feasible fixed points*, denoted L and R, and defined, respectively, as

$$L: \quad (x,y) = (x_L^*, y^*) \in D_L, \tag{8}$$
$$R: \quad (x,y) = (x_R^*, y^*) \in D_R,$$

---

[4]A trangular map has the following structure: $(x',y') = (f(x,y), g(y))$.

where

$$x_L^* = \frac{wc}{y^* + \delta - ra}, \quad x_R^* = \frac{w(b+c)}{y^* + \delta}, \quad y^* = 1 - \frac{1}{\mu}. \tag{9}$$

In fact, from $f(y) = y$ we get two solutions, $y = 0$ and $y = y^*$. Given that only positive values of the variables are feasible, the first solution is not considered here (it leads to saddle fixed points on the boundary of the feasible region). Substituting $y = y^*$ first to $G_L(x, y) = x$ and then to $G_R(x, y) = x$, we get x_L^* and x_R^*, respectively, so that the points L and R are the fixed points of maps T_L and T_R. Obviously, L and R are really existing fixed points of T only if they belong to their definition regions, that is, if $0 < x_L^* \leq b/a$ and $x_R^* > b/a$, that holds for the following parameter regions:

$$P_L = \left\{ p : w \leq \frac{b(y^* + \delta - ra)}{ac}, \ y^* + \delta - ra > 0 \right\},$$

$$P_R = \left\{ p : w > \frac{b(y^* + \delta)}{a(b+c)} \right\},$$

respectively, where p denotes a point in the parameter space satisfying (7). The boundaries

$$\xi_L = \left\{ p : w = \frac{b(y^* + \delta - ra)}{ac} \right\}, \tag{10}$$

$$\xi_R = \left\{ p : w = \frac{b(y^* + \delta)}{a(b+c)} \right\}, \tag{11}$$

at which $x_L^* = b/a$ and $x_R^* = b/a$, respectively, are related to the BCB of the fixed points L and R.

It is easy to see that for $p \in P_L$ ($p \in P_R$) the fixed point L (resp., R) is an *attracting node* if $\mu \in I_1$ where $I_1 = (1, 3)$, and a *saddle* if $\mu > 3$. In fact, except for the points of the discontinuity line C_{-1} on which Jacobian is not defined, that is, $x_0 \neq b/a$, the eigenvalues of the Jacobian matrix of map T evaluated at any point (x_0, y_0) are

$$\lambda_h(x_0, y_0) = \begin{cases} s_L = \dfrac{1 - \delta + ra}{1 + y_0}, & x_0 < \dfrac{b}{a}, \\ s_R = \dfrac{1 - \delta}{1 + y_0}, & x_0 > \dfrac{b}{a}, \end{cases}$$

and

$$\lambda_v(x_0, y_0) = f'(y_0) = \mu(1 - 2y_0),$$

related to the horizontal and vertical eigendirections (typical for triangular 2D maps), respectively. For the fixed points L and R we have

$$\lambda_h(L) = \frac{1 - \delta + ra}{1 + y^*}, \quad \lambda_v(L) = 2 - \mu,$$

$$\lambda_h(R) = \frac{1 - \delta}{1 + y^*}, \quad \lambda_v(R) = 2 - \mu.$$

For parameters $p \in P_L$ the inequality $0 < \lambda_h(L) < 1$ holds, and if $p \in P_R$ then $0 < \lambda_h(R) < 1$, while $|\lambda_v(L)| = |\lambda_v(R)| < 1$ for $\mu \in I_1$. That is, the existing fixed point, L or R, of map T is always attracting in the horizontal direction, while in the vertical direction it is attracting for $\mu \in I_1$ and repelling for $\mu > 3$. This implies that the asymptotic dynamics of the 2D map T for $\mu \in I_1$ is governed by the 1D discontinuous piecewise linear map already studied in detail in [14]. In the next section we recall some results related to this map and describe the bifurcation structure of the (r, w)-parameter plane for $\mu \in I_1$.

4 Reduction to a 1D piecewise linear map with one discontinuity

From the remarks of the previous section we can state the following

4

Proposition 1. *For $\mu \in I_1$ where $I_1 = (1, 3)$, any orbit of map T with initial condition $(x_0, y_0) \in \mathbb{R}_+^2$ is attracted to the invariant line*

$$L^* = \left\{ (x, y) \in \mathbb{R}_+^2 : \; y = y^* \right\}, \tag{12}$$

where $y^* = 1 - 1/\mu$, on which T is reduced to a 1D discontinuous piecewise linear map $g : \mathbb{R}_+ \to \mathbb{R}_+$ defined as follows:

$$g : x \mapsto g(x) = \begin{cases} g_L(x) = \dfrac{(1 - \delta + ra)\, x + wc}{1 + y^*} & \text{if} \quad x \leq \dfrac{b}{a}, \\[3mm] g_R(x) = \dfrac{(1 - \delta)\, x + w(b + c)}{1 + y^*} & \text{if} \quad x < \dfrac{b}{a}. \end{cases} \tag{13}$$

For $\mu \in I_1$ the logistic map f has a repelling fixed point $y = 0$, an attracting fixed point $y = y^*$ and no other invariant set. Thus, any orbit of T with an initial point $(x_0, y_0) \in \mathbb{R}_+^2$ is attracted to the invariant line L^* (called layer) associated with the attracting fixed point $y = y^*$.

Obviously, for the 2D map T the layer L^* remains invariant also for $\mu > 3$, and the restriction of T to the layer is always the map g defined in (13), but in such a case L^* is transversely repelling.

The map g belongs to the class of 1D discontinuous piecewise increasing maps studied by many researchers (see, e.g., [29], [30], [31], [32], [20]). One of the characteristic features of such maps, when they are invertible on the absorbing interval, is the *period adding structure* observed in the parameter space. It is formed by periodicity regions which are ordered according to the following rule (also called Farey summation rule): between any two periodicity regions related to attracting cycles with rotation numbers m_1/n_1 and m_2/n_2 there is a region related to attracting cycles with rotation number $m_3/n_3 = (m_1 + m_2)/(n_1 + n_2)$. In the piecewise linear case all the boundaries of these periodicity regions can be obtained analytically (see [29], [18], [19]).

In [14] the period adding structure of map g is described in the (r, w)-parameters plane. In the figures of the present paper we fix the parameters a, b, c and δ as in [14], that is,

$$a = 1.5, \;\; b = c = 2.9, \;\; \delta = 0.45 \tag{14}$$

and study dynamics of T depending on the parameters r, w and μ (as $y^* = 1 - 1/\mu$, y^* can take values in the range $(0, 2/3)$ while in [14] it was considered $y^* = 0.45$ fixed).

Let $\{x_i\}_{i=1}^n$ be the points of an n-cycle of map g, then its symbolic representation can be written as $\sigma = s_1 s_2 ... s_n$ where each symbol $s_i \in \{L, R\}$ is associated with the point x_i depending on whether x_i is on the left or on the right of the border point $x = b/a$. That is, s_i is set equal to L if $x_i < b/a$ and to R if $x > b/a$. To denote an n-cycle of map g we use its symbolic representation. Cycles LR^n and RL^n, $n \geq 1$, are called *basic cycles*. They belong to two families of complexity level one according to [29]. In Appendix we recall how to get cycles of higher complexity levels forming the period adding structure, as well as how to determine the equations of the related BCBs. An example of the graph of map g is shown in Fig.1, together with its absorbing interval

$$I = [g_R(b/a), g_L(b/a)] \tag{15}$$

and an attracting 3-cycle RL^2 which is the unique attractor at the given parameter values.

In Fig.2 we show a 2D bifurcation diagram of map T in the (r, w)-parameter plane for $\mu = 2$. In this diagram the periodicity regions corresponding to attracting cycles of different periods are shown by different colors, where the correspondence between the color and the period is given in the color bar (some periods are indicated also by numbers).

According to Proposition 1 this bifurcation structure can be explained by means of map g where $y^* = 0.5$. Note that map g is invertible on the absorbing interval I if $g_R(g_L(b/a)) < g_L(g_R(b/a))$ and noninvertible otherwise, so that the transition between invertible and noninvertible occurs at the boundary defined by the equation $g_R(g_L(b/a)) = g_L(g_R(b/a))$, that holds for

$$\kappa = \left\{ p : w(ra(c + b) - b(y^* + \delta)) = 0 \right\}. \tag{16}$$

The set κ is defined by two subsets, $\kappa_1 = \{p : w = 0\}$ and $\kappa_2 = \{p : ra(c+b) - b(y^* + \delta) = 0\}$. Given that we consider $w > 0$, map g is invertible on I for $ra(c+b) - b(y^* + \delta) > 0$. In the (r, w)-parameter plane shown in Fig.2 the set κ_2 (defined by $r = b(y^* + \delta)/a(c + b) \approx 0.3167$) is the vertical line through the point $\xi_L \cap \xi_R$.

Figure 1: Graph of map g given in (13), its absorbing interval $I = [g_R(b/a), g_L(b/a)]$ and its attracting 3-cycle RL^2. Here $y^* = 0.5$ ($\mu = 2$), $r = 0.7$, $w = 0.15$ and the other parameters fixed as in (14).

Figure 2: 2D bifurcation diagram of the map T in the (r, w)-parameter plane for $\mu = 2$. The other parameters are fixed as in (14).

As discussed in [20], an intersection point of two BCB curves of different attracting fixed points (or cycles) of a 1D piecewise increasing discontinuous map, when the map is invertible on the absorbing interval, is an issue point of a full period adding structure. In Fig.2 we see this structure issuing from the intersection point of the curves ξ_L and ξ_R, defined in (10) and (11), which are the BCB curves of the fixed points L and R of map T, as well as the BCB curves of the fixed points x_L^* and x_R^* of map g. In Appendix, following [14], we recall how all the cycles associated with the period adding structure are grouped according to their complexity levels, as well as how to get analytically the boundaries of the related parameter regions.

5   Dynamics of T on two cyclic layers

As we have seen (Proposition 1), for $\mu \in I_1$ the asymptotic dynamics of T belong to the layer L^*, and it is known that at $\mu = 3$ the fixed point y^* of the logistic map f undergoes a flip bifurcation, leading to a 2-cycle $\{y_1, y_2\}$ where

$$y_{1,2} = \frac{\mu + 1 \pm \sqrt{\mu^2 - 2\mu - 3}}{2\mu},\tag{17}$$

6

which is attracting for $\mu \in I_2$ where $I_2 = (3, 1 + \sqrt{6})$. In this section we consider the dynamics of T when μ belongs to this interval.

In Fig.3 we show the bifurcation structure of the (w, μ)-parameter plane at $r = 0.53$ and other parameters fixed as in (14). In the parameter region with $\mu \in I_1$ one can seen the period adding bifurcation structure that can be completely described by means of map g considered in the previous section. In the present one we describe how this structure is modified in the parameter region with $\mu \in I_2$ (while the description of the bifurcation occurring for T at $\mu = 3$ is presented after).
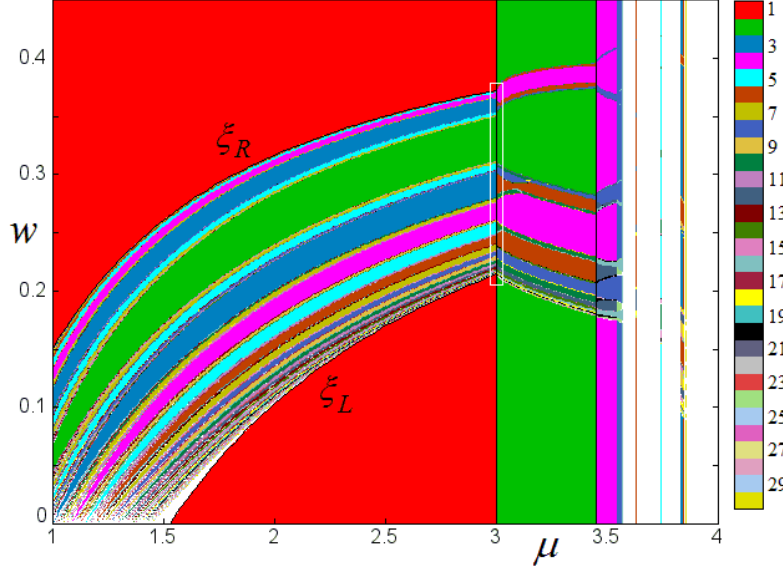
Figure 3: 2D bifurcation diagram of map T in the (w, μ)-parameter plane at $r = 0.53$. The other parameters are fixed as in (14). An enlargement of window indicated by white lines is shown in Fig.7.

So, for $\mu \in I_2$ the logistic map f has an attracting 2-cycle, and for 2D map T this leads to the existence, for $\mu > 3$, of two straight lines (layers):

$$L_1 = \left\{ (x, y) \in \mathbb{R}_+^2 : \ y = y_1 \right\} \text{ and } L_2 = \left\{ (x, y) \in \mathbb{R}_+^2 : \ y = y_2 \right\}, \tag{18}$$

which are cyclical for T and invariant for the second iterate of the map, T^2. Moreover, these layers are transversely attracting for $\mu \in I_2$. So, the following proposition holds:

Proposition 2. For $\mu \in I_2$ where $I_2 = (3, 1 + \sqrt{6})$, any orbit of map T with an initial point $(x_0, y_0) \in \mathbb{R}_+^2$ (except for the points belonging to the layer L^*, given in (12), and all its preimages by T) is attracted to the 2-cyclical layers $\{L_1, L_2\}$ given in (18). On L_1 the map T^2 is reduced to a 1D discontinuous piecewise linear map $g_1 : \mathbb{R}_+ \to \mathbb{R}_+$ defined as follows:

$$g_1 : x \mapsto g_1(x) = \begin{cases} g_{LL}(x) = G_L(G_L(x, y_1), y_2), & x \leq \min\left\{\dfrac{b}{a}, \overline{x_1}\right\}, \\[2mm] g_{LR}(x) = G_R(G_L(x, y_1), y_2), & \overline{x_1} < x \leq \dfrac{b}{a}, \\[2mm] g_{RL}(x) = G_L(G_R(x, y_1), y_2), & \dfrac{b}{a} < x \leq \overline{x_2}, \\[2mm] g_{RR}(x) = G_R(G_R(x, y_1), y_2), & x > \max\left\{\dfrac{b}{a}, \overline{x_2}\right\}, \end{cases} \tag{19}$$

where $G_L(x, y_1) = \dfrac{(1 - \delta + ra)\, x + wc}{1 + y_1}$, $G_R(x, y_1) = \dfrac{(1 - \delta)\, x + w(b + c)}{1 + y_1}$,

$$\overline{x_1} = \dfrac{b(1 + y_1) - awc}{a(1 - \delta + ra)}, \qquad \overline{x_2} = \dfrac{b(1 + y_1) - aw(b + c)}{a(1 - \delta)},$$

and y_1, y_2 are given in (17). Similarly, on the layer L_2 the map T^2 is reduced to a 1D discontinuous piecewise linear map $g_2 : \mathbb{R}_+ \to \mathbb{R}_+$ given by function $g_2(x)$ which is defined replacing y_1 by y_2 and vice versa in (19).

The map g_1 can have at most four linear branches (with positive slopes) and at most three discontinuity points. The first discontinuity point is the same as in map g, that is, $x = b/a$, and from $G_L(x, y_1) = b/a$ and $G_R(x, y_1) = b/a$ we obtain two more discontinuity points, $\overline{x_1}$ and $\overline{x_2}$. Two examples of map g_1 are shown in Fig.4, namely, in Fig.4a map g_1 is defined by three branches and has an attracting 2-cycle, while in Fig.4b map g_1 is given by four branches and has two coexisting fixed points.
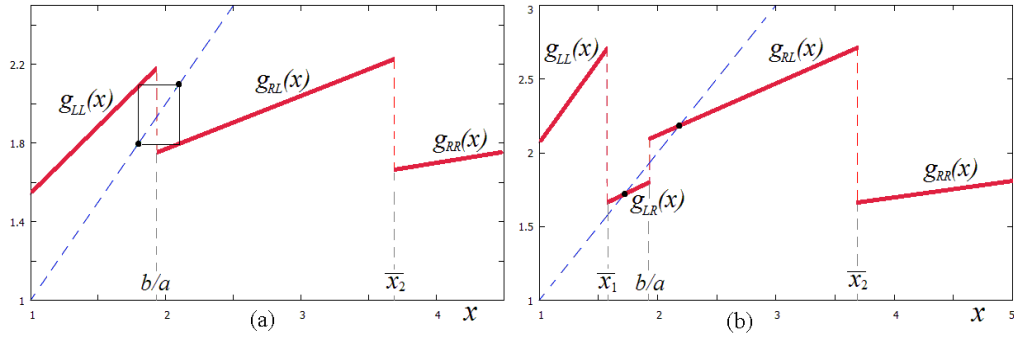
Figure 4: The map g_1 given in (19) and its (a) attracting 2-cycle for $\mu = 3.2$, $r = 0.55$, $w = 0.25$; (b) two coexisting fixed points for $\mu = 3.2$, $r = 0.8$, $w = 0.25$.

It is clear that the overall bifurcation structure of a 1D discontinuous piecewise linear map with more than one discontinuity point is more complicated than the one of the map with one discontinuity. In fact, the description of such a structure in the generic case it is still an open problem (see e.g. [21], [33], [34] where some particular cases are studied). Clearly, as a starting point of investigation of the bifurcation structure one can search for a parameter region corresponding to only two linear branches involved in asymptotic dynamics (or, in other words, in the absorbing interval). That is, only one discontinuity point belongs to the absorbing interval of the map, as it occurs in Fig.4a,b. In such a region we can expect to observe the period adding structure already discussed in the previous section. In fact, in Fig.5 we present the 2D bifurcation diagram of map g_1 in the (r, w)-parameter plane for $\mu = 3.2$, where one can see two period adding structures issuing from the points indicated by black circles. We can explain why the period adding structures are issuing from these points.

As we show below, the black circles in Fig.5 are the intersection points of BCB curves of different fixed points of map g_1. To get these curves we first obtain the possible fixed points of map g_1, denoted x^*_{LL}, x^*_{LR}, x^*_{RL} and x^*_{RR}, solving the equations $g_{LL}(x) = x$, $g_{LR}(x) = x$, $g_{RL}(x) = x$ and $g_{RR}(x) = x$, respectively. These points are true fixed points of g_1 only if they belong to the definition intervals of the related linear branches. The collision of a fixed point with a border of the related interval leads to the condition of its appearance/disappearance, that is, the condition of its BCB. In Fig.5 the following BCB curves are shown:

$$\xi^{b/a}_{LL} = \{p : x^*_{LL} = b/a\}, \quad \xi^{\overline{x_2}}_{RR} = \{p : x^*_{RR} = \overline{x_2}\}, \tag{20}$$

$$\xi^{b/a}_{RL} = \{p : x^*_{RL} = b/a\}, \quad \xi^{\overline{x_2}}_{RL} = \{p : x^*_{RL} = \overline{x_2}\}, \tag{21}$$

$$\xi^{\overline{x_1}}_{LR} = \{p : x^*_{LR} = \overline{x_1}\}, \quad \xi^{b/a}_{LR} = \{p : x^*_{LR} = b/a\}. \tag{22}$$

The attracting fixed point x^*_{LL} exists below the curve $\xi^{b/a}_{LL}$ related to its BCB with the border point $x = b/a$; the attracting fixed point x^*_{RR} exists above the curve $\xi^{\overline{x_2}}_{RR}$ related to its BCB with $x = \overline{x_2}$; the attracting fixed point x^*_{RL} exists above the curve $\xi^{b/a}_{RL}$ (BCB with $x = b/a$) and below $\xi^{\overline{x_2}}_{RL}$ (BCB with $x = \overline{x_2}$), and, finally, the attracting fixed point x^*_{LR} exists above the curve $\xi^{\overline{x_1}}_{LR}$ (BCB with $x = \overline{x_1}$) and below $\xi^{b/a}_{LR}$ (BCB with $x = b/a$). Note that the existence regions of x^*_{RL} and x^*_{LR} are overlapped, so that in the dashed region x^*_{LR} coexists with x^*_{RL}, as in the example shown in Fig.4b.
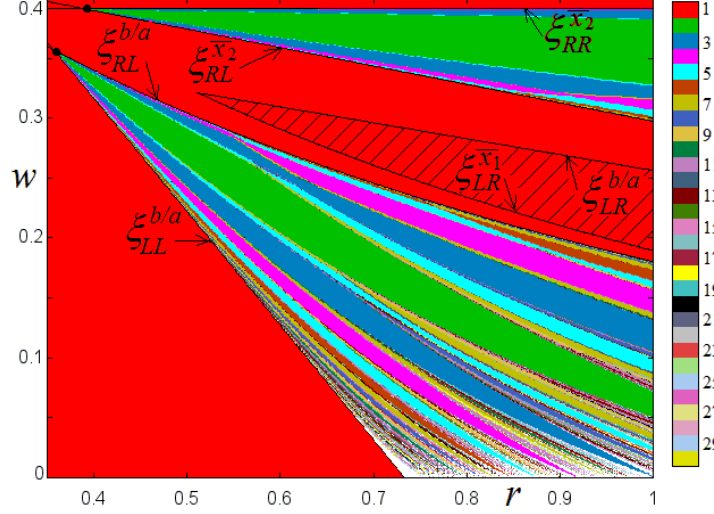
Figure 5: 2D bifurcation diagram of the map g_1 in the (r, w)-parameter plane for $\mu = 3.2$ and the other parameters as in (14).

It is easy to check that for the parameter values related to the point $p_1 = \xi_{LL}^{b/a} \cap \xi_{RL}^{b/a}$ the map g_1 is continuous at the border point $x = b/a$, and thus we can state (see [20]) that this point is an issue point of the period adding structures associated with the branches $g_{LL}(x)$ and $g_{RL}(x)$ of map g_1. Similarly, we can state that one more period adding structures is associated with the branches $g_{RL}(x)$ and $g_{RR}(x)$, issuing from the point $p_2 = \xi_{RL}^{\overline{x_2}} \cap \xi_{RR}^{\overline{x_2}}$ at which map g_1 is continuous at $x = \overline{x_2}$. These two period adding structures are observed in Fig.5, and the formulas of the boundaries of the related periodicity regions can be obtained following the approach described in Appendix.

Coming back to the 2D map T, we recall that map g_1 represents a reduction of T^2 on the layer L_1. Thus, an n-cycle of map g_1 leads to the existence of a $2n$-cycle of map T (with periodic points which alternate on the two layers L_1 and L_2 given in (18)). That is, with regards to map T all the periodicity regions of n-cycles in Fig.5 are related to attracting cycles of T of doubled periods $2n$. For example, for parameter values related to two coexisting fixed points of map g_1 presented in Fig.4b, map T has two coexisting 2-cycles indicated in Fig.6 by black and gray circles. It is also shown by white circles a saddle 2-cycle belonging to the layer L^* given in (12) associated with a 2-cycle of map g defined in (13).

The basins of the coexisting attracting 2-cycles, shown in red and white in Fig.6, are separated by the discontinuity line C_{-1} $(x = b/a)$ and all its preimages (not horizontal basin boundaries), as well as by the layer L^* and all its preimages which are horizontal lines accumulating towards $\{(x, y) : y = 0\}$ and $\{(x, y) : y = 1\}$, associated with the repelling fixed point $y = 0$ of the logistic map f and its preimage $y = 1$. That is, the values of y at which we have these horizontal lines are given by all the preimages of the fixed point $y = y^* = 1 - 1/\mu$ of the logistic map f.

6 Bifurcation of cycles of T at $\mu = 3$

As already remarked, for $\mu \in I_1$ the map T on the layer L^* (when a fixed point does not exist) can have an attracting cycle of any symbolic sequence according to the period adding structure, as well as aperiodic trajectories, depending on the dynamics of the 1D discontinuous map g. More precisely, in the generic case the (unique) attractor of T is either the fixed point $L(x_L^*, y^*)$, or the fixed point $R(x_R^*, y^*)$, or an n-cycle $\gamma_n = \{(x_i, y^*)\}_{i=0}^{n-1}$, $n \geq 2$. In a nongeneric case the attractor of T is a quasiperiodic orbit on L^* (it occurs for a zero-measure set of parameter values, see [19]). Now we turn to describe which bifurcation occurs for T at $\mu = 3$, that is, if μ increases through $\mu = 3$.

Let us first consider an enlargement of Fig.3, presented in Fig.7. It can be seen that if μ passes through
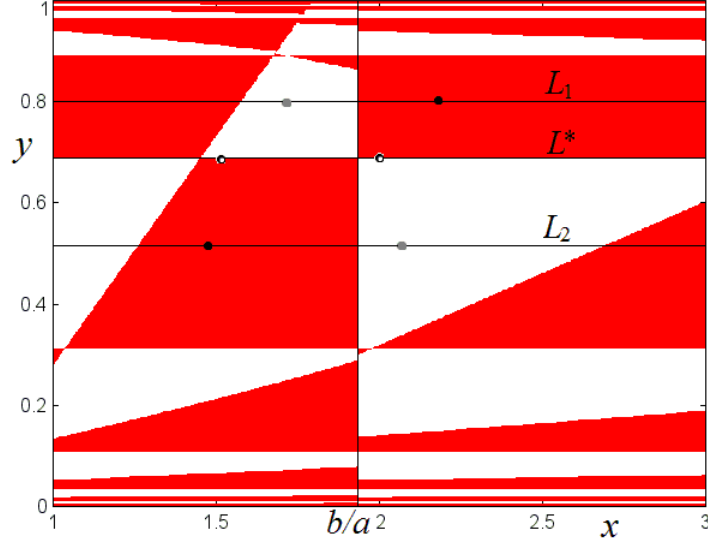
9

Figure 6: Two coexisting attracting 2-cycles (black and gray circles) of the map T and their basins of attraction for $\mu = 3.2$, $r = 0.8$, $w = 0.25$.

$\mu = 3$ then cycles of even periods lead to cycles of the same period (but, as we show, not unique), while cycles of odd periods lead to (unique) cycles of double periods. In Fig.7 we show also the BCB curves defined in (20), (21) and (22), which are related to BCBs of the attracting fixed points of map g_1 which correspond, for map T, to BCBs of the related attracting 2-cycles. In particular, one can see that for the parameter values belonging to the dashed region, map T has two coexisting attracting 2-cycles. In fact, as we see below, for μ in a right neighborhood of $\mu = 3$ two cycles of even period must coexist.

Proposition 3. *Let γ_n be an n-cycle of map T existing on the layer L^* for $\mu < 3$. Then, at $\mu = 3$ the cycle γ_n undergoes:*

- *a flip bifurcation leading to a unique cycle of double period if n is odd,*

- *a pitchfork bifurcation leading to a pair of n-cycles if n is even,*

with periodic points belonging to the layers L_1 and L_2 given in (18).

In fact, if we consider an n-cycle γ_n of map T related to the cycle $\{x_i\}_{i=0}^{n-1}$ of map g with symbolic sequence σ, then the eigenvalues of γ_n are

$$\lambda_h(\gamma_n) = s_L^m s_R^{n-m} = \left(\frac{1 - \delta + ra}{1 + y^*}\right)^m \left(\frac{1 - \delta}{1 + y^*}\right)^{n-m} \tag{23}$$

where m is the number of symbols L in σ, and

$$\lambda_v(\gamma_n) = (f'(y^*))^n = (2 - \mu)^n. \tag{24}$$

For $\mu \in I_1$ the cycle γ_n is attracting with $0 < \lambda_h(\gamma_n) < 1$, and $|\lambda_v(\gamma_n)| < 1$. At $\mu = 3$ we have $\lambda_v(\gamma_n) = 1$ if n is even, so that the n-cycle γ_n undergoes *pitchfork bifurcation* leading to two attracting n-cycles, while $\lambda_v(\sigma) = -1$ if n is odd, so that σ undergoes *period-doubling bifurcation* leading to an attracting $2n$-cycle.

As it can be seen also from Fig.7, increasing μ one of the coexisting n-cycles appearing when n is even can disappear due to a BCB. This can be clearly seen to occur with the 2-cycle of map T in the same figure, where the BCB curves are shown and the region of coexistence is evidenced. If the parameter point crosses the boundary $\xi_{LR}^{\overline{x_1}}$ or $\xi_{LR}^{b/a}$ of the dashed region in Fig.7 then one of the attracting 2-cycles disappears. A similar behavior occurs inside all the periodicity regions associated with a pair of cycles of even periods.
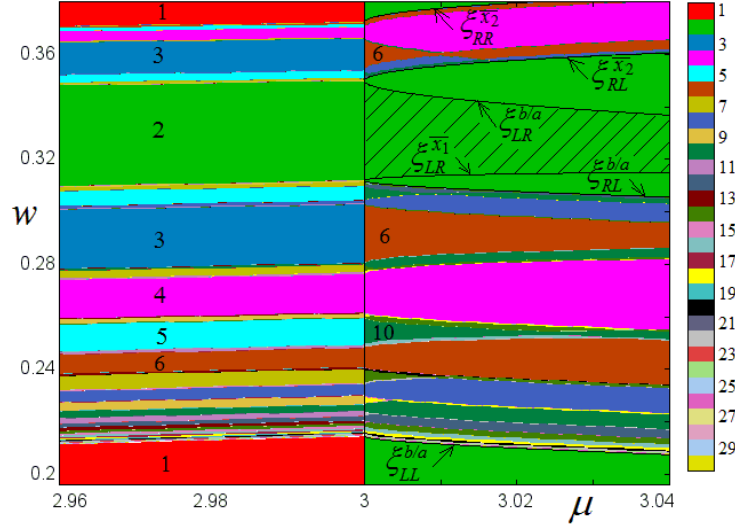
Figure 7: An enlargement of the window indicated in Fig.3.

It is easy to see that a similar reasoning can be used to describe the bifurcation occurring at $\mu = 1 + \sqrt{6} \approx 3.449499$, which is the flip bifurcation value of the 2-cycle of the logistic map f, leading to an attracting 4-cycle, say, with periodic points y_i, $i = 1, 2, 3, 4$. Thus, for the 2D map T all the periodic points and asymptotic dynamics belong to four cyclic invariant layers defined by $y = y_i$, $i = 1, 2, 3, 4$. For μ in a left neighborhood of $\mu = 1 + \sqrt{6}$ all the cycles have even periods, some are multiple of 4 and some are not. Thus at the bifurcation occurring for $\mu = 1 + \sqrt{6} \approx 3.449499$ any cycle having period multiple of 4 undergoes a pitchfork bifurcation and leads to coexistence of cycles of the same period, while the cycle whose period is not multiple of 4 undergoes a flip bifurcation leading to a cycle of double period. Thus in a right neighborhood of $\mu = 1 + \sqrt{6}$ all the cycles have a period which is multiple of 4.
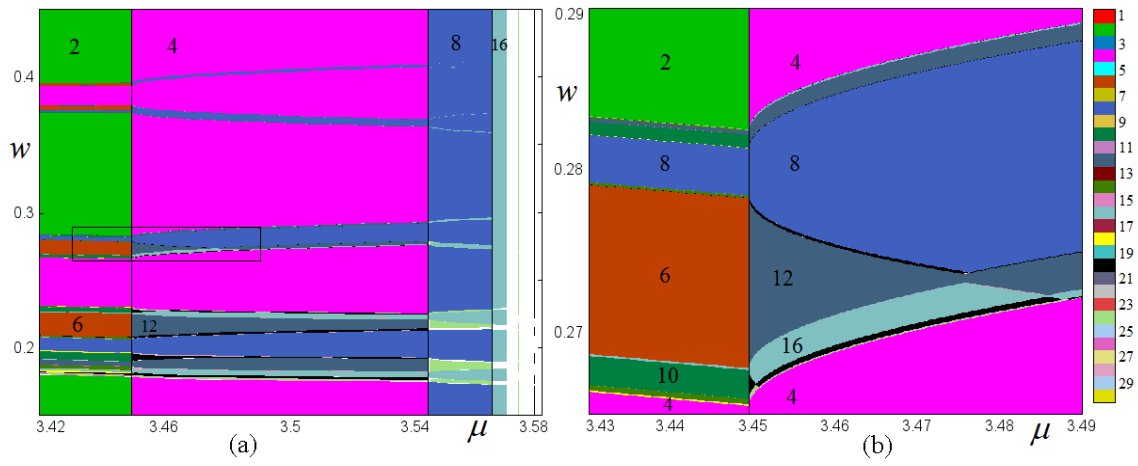

Figure 8: In (a): an enlarged part of the 2D bifurcation diagram of map T shown in Fig.3; in (b): an enlargement of the window indicated in (a).

The attracting 4-cycle of map f undergoes a period-doubling bifurcation at $\mu \approx 3.544090$, and so on. It is well known that in the logistic map f the first period-doubling cascade is observed for $3 < \mu < \mu^*$, where $\mu^* \approx 3.569946$ is Feigenbaum accumulation point, and for each bifurcation value we can reason similarly for the 2D map T. In correspondence to this cascade we see in Fig.3 and in its enlargement shown in Fig.8a

11

a sequence of windows of decreasing width, related to attracting cycles whose periods are either doubled (a period-doubling bifurcation occurs), or remain the same (a pitchfork bifurcation occurs).

It is well known that for $\mu > \mu^*$ the logistic map is chaotic (an invariant set with chaotic dynamics exists), although periodic windows of any period also exist (see [35]). In particular, map f has a *chaotic attractor* (in one interval or in cyclical intervals) for a completely disconnected set (of positive Lebesgue measure) of values of μ from the interval $\mu^* < \mu \leq 4$, while for almost all other values of μ map f has an attracting cycle coexisting with a *chaotic repellor*. These results can be applied to map T accordingly, in particular, one can state that for $\mu > \mu^*$ the map T is chaotic.

7   Conclusion

The quest for growth models endogenously generating business cycles is a long standing one. In the early years of economic growth theory economists obtained endogenous fluctuations by adding more structure to the simpler base models, for instance by considering more than one sector.

In this paper we have studied the dynamic behavior occurring in a model recently proposed in [17], where both discontinuity and nonlinearity are present. The system is described by a 2D discontinuous map characterized by a piecewise linear function and a smooth one. We have shown that also in such a 2D maps the period adding structure can occur, leading to attracting cycles of specific periods. The border collision bifurcation boundaries of periodicity regions related to attracting cycles can also be determined analytically, by using the formulas presented in Appendix. Moreover, we have found the new interesting scenarios of bistability which may occur in parameters' regions that are not negligible, and in correspondence of particular bifurcation values.

Given that the sources of nonlinearities and switching regimes in economics (as well as in other disciplines) are quite numerous, we hope that the study of this kind of dynamical systems will proceed in order to better understand all the implications of such structures.

References

[1] J. Benhabib, K. Nishimura, Competitive equilibrium cycles, J. Econ. Theory 35 (1985) 284-306.

[2] M. Boldrin, L. Montrucchio, On the indeterminacy of capital accumulation paths, J. Econ. Theory 40 (1986) 26-39.

[3] R.H. Day, Irregular growth cycles, Am. Econ. Rev. 72 (1982) 406-414.

[4] R.H. Day, The emergence of chaos from classical economic growth, Q. J. Econ. 98 (1983) 201-213.

[5] J.G. Brida, E. Accinelli, The Ramsey model with logistic population growth, Econ. Bull. 3 (2007) 1-8.

[6] L. Guerrini, The Solow-Swan model with a bounded population growth rate, J. Math. Econ. 42 (2006) 14-21.

[7] L. Guerrini, The Ramsey model with a bounded population growth rate, J. Macroecon. 32 (2010) 872-878.

[8] L. Guerrini, A closed-form solution to the Ramsey model with logistic population growth, Econ. Model. 27 (2010) 1178-1182.

[9] L. Guerrini, The Ramsey model with AK technology and a bounded population growth rate, J. Macroecon. 32 (2010) 1178-1183.

[10] L. Guerrini, Transitional dynamics in the Ramsey model with AK technology and logistic population change, Econ. Lett. 109 (2010) 17-19.

[11] J.G. Brida, D. Ritelli, G.M. Scarpello, The Solow model with logistic manpower: a stability analysis, J. World Econ. Rev. 3 (2008) 161-166.

[12] S. Brianzoni, C. Mammana, E. Michetti, Nonlinear dynamics in a business-cycle model with logistic population growth, Chaos, Solitons & Fractals 40 (2009) 717-730.

[13] V. Böhm, L. Kaas, Differential savings, factor shares, and endogenous growth cycles, J. Econ. Dyn. Control 24 (2000) 965-980.

[14] F. Tramontana, L. Gardini, A. Agliari, Endogenous cycles in discontinuous growth models, Math. Comput. Simul. 81 (2011) 1625–1639.

[15] K. Matsuyama, Growing through cycles, Econometrica 67 (1999) 335–347.

[16] L. Gardini, I. Sushko, A.K. Naimzada, Growing through chaotic intervals, J. Econ. Theory 143 (2008) 541–557.

[17] F. Tramontana, V. Avrutin, V., 2014. Complex endogenous dynamics in a one-sector growth model with differential savings. Working Paper of the Department of Economics and Management, University of Pavia (Italy).

[18] V. Avrutin, M. Schanz, L. Gardini, Calculation of bifurcation curves by map replacement, Intern. J. Bifurc. Chaos 20 (2010) 3105-3135.

[19] L. Gardini, F. Tramontana, V. Avrutin, M. Schanz, Border Collision Bifurcations in 1D PWL map and Leonov's approach, Intern. J. Bifurc. Chaos 20 (2010) 3085-3104.

[20] L. Gardini, V. Avrutin, I. Sushko, Codimension-2 border collision bifurcations in one-dimensional discontinuous piecewise smooth maps, Intern. J. Bifurc. Chaos 24 (2014) 1450024 (30 pages).

[21] F. Tramontana, L. Gardini, V. Avrutin, M. Schanz, Period Adding in Piecewise Linear Maps with Two Discontinuities, Intern. J. Bifurc. Chaos 22 (2012) 1250068 (30 pages)

[22] A. Panchuk, I. Sushko, B. Schenke, V. Avrutin, Bifurcation Structures in a Bimodal Piecewise Linear Map: Regular Dynamics. Intern. J. Bifurc. Chaos 23 (2013) 1330040.

[23] C. Mira, Embedding of a Dim 1 piecewise continuous and linear Leonov map into a Dim 2 invertible map, in: G.I. Bischi, C. Chiarella, I. Sushko (Eds.), Global Analysis of Dynamic Models in Economics and Finance, Springer Verlag, New York, 2013.

[24] N. Kaldor, Alternative theories of distribution, Rev. Econ. Stud. 23 (1956) 83-100.

[25] N. Kaldor, A model of economic growth, Econ. J. 67 (1957) 591-624.

[26] L. Pasinetti, Rate of profit and income distribution in relation to the rate of economic growth, Rev. Econ. Stud. 29 (1962) 267-279.

[27] Y.L. Maistrenko, V.L. Maistrenko, L.O. Chua, Cycles of chaotic intervals in a time-delayed Chua's circuit, Intern. J. Bifurc. Chaos 3 (1993) 1557–1572.

[28] I. Sushko, L. Gardini, Degenerate bifurcations and border collisions in piecewise smooth 1D and 2D maps, Intern. J. Bifurc. Chaos 20 (2010) 2045–2070.

[29] N.N. Leonov, Map of the line onto itself, Radiofisika 3 (1959) 942–956.

[30] J.P. Keener, Chaotic behavior in piecewise continuous difference equations, Trans. Am. Math. Soc. 261 (1980) 589–604.

[31] A.J. Homburg, Global aspects of homoclinic bifurcations of vector fields, Memories of the American Math. Soc., Vol. 578, Springer, Heidelberg, 1996.

[32] P.L. Boyland, Bifurcations of circle maps: Arnold tongues, bistability and rotation intervals, Commun. Math. Phys. 106 (1986) 353-381.

[33] F. Tramontana, F. Westerhoff, L. Gardini, One-dimensional maps with two discontinuity points and three linear branches: mathematical lessons for understanding the dynamics of financial markets, Decis. Econ. Financ. 37 (2014) 27–51.

[34] F. Tramontana, F. Westerhoff, L. Gardini, A simple financial market model with chartists and fundamentalists: market entry levels and discontinuities, Math. Comput. Simul. 2014 (to appear).

[35] C. Mira, Chaotic Dynamics, World Scientific, Singapore, 1987.

[36] C. Mira, L. Gardini, A. Barugola, J.C. Cathala, Chaotic Dynamics in Two-Dimensional Nonivertible Maps, Nonlinear Sciences, Series A, World Scientific, Singapore, 1996.

Appendix (Period adding structure)

Consider a generic family of 1D discontinuous piecewise linear maps $q : \mathbb{R} \to \mathbb{R}$ with one border point $x = d$, defined as

$$q : x \mapsto q(x) = \begin{cases} q_L(x) = a_L x + \mu_L & \text{if } x < d, \\ q_R(x) = a_R x + \mu_R & \text{if } x > d. \end{cases} \tag{25}$$

It is known (see, e.g., [18], [19], [21], [22]) that period adding structure is observed in the parameter space of map q if $a_L > 0$, $a_R > 0$, $q_R(d) < d < q_L(d)$ and map q is invertible on the absorbing interval $I = [q_R(d), q_L(d)]$, that holds for $q_R(q_L(d)) < q_L(q_R(d))$.

Following [29], all the cycles associated with the period adding structure are grouped into families according to *complexity levels*. The *complexity level one* includes two families, denoted $\Sigma_{1,1}$ and $\Sigma_{2,1}$, to which the so-called *basic* cycles belong:

$$\Sigma_{1,1} = \{LR^{n_1}\}_{n_1=1}^{\infty}, \quad \Sigma_{2,1} = \{RL^{n_1}\}_{n_1=1}^{\infty}. \tag{26}$$

To get the symbolic sequences of the cycles of families of *complexity level two* we apply to the families $\Sigma_{1,1}$ and $\Sigma_{2,1}$ the following *symbolic replacements:*

$$\kappa_m^L := \begin{cases} L \to LR^m \\ R \to RLR^m \end{cases}, \quad \kappa_m^R := \begin{cases} L \to LRL^m \\ R \to RL^m \end{cases} \tag{27}$$

(see [18], [19]). Namely, at first we substitute in $\Sigma_{1,1}$ each symbol L by LR^m and each symbol R by RLR^m (replacement κ_m^L), and then we substitute in $\Sigma_{1,1}$ each symbol L by LRL^m and each symbol R by RL^m (replacement κ_m^R). Then setting the index $m = n_2$ we get the two families of complexity level two:

$$\Sigma_{1,2} = \{LR^{n_2}(RLR^{n_2})^{n_1}\}_{n_1,n_2=1}^{\infty}, \quad \Sigma_{2,2} = \{LRL^{n_2}(RL^{n_2})^{n_1}\}_{n_1,n_2=1}^{\infty}. \tag{28}$$

Similarly, applying the replacements κ_m^L and κ_m^R to $\Sigma_{2,1}$ we get the symbolic sequences of two more families:

$$\Sigma_{3,2} = \{RLR^{n_2}(LR^{n_2})^{n_1}\}_{n_1,n_2=1}^{\infty}, \quad \Sigma_{4,2} = \{RL^{n_2}(LRL^{n_2})^{n_1}\}_{n_1,n_2=1}^{\infty}. \tag{29}$$

In short, this procedure can be written as $\Sigma_{1,2} = \kappa_{n_2}^L(\Sigma_{1,1})$, $\Sigma_{2,2} = \kappa_{n_2}^R(\Sigma_{1,1})$, $\Sigma_{3,2} = \kappa_{n_2}^L(\Sigma_{2,1})$ and $\Sigma_{4,2} = \kappa_{n_2}^R(\Sigma_{2,1})$. So, we get 4 families of complexity level two[5]. Further, applying the replacements (27)

---

[5] One more way to construct the families of the complexity level two consists in consecutive concatenation of the 'neighbor' symbolic sequences of the first complexity level. As shown in [18], the symbolic sequences obtained in such a way are shift invariant to those obtained by the symbolic replacements (27).

with $m = n_3$ to the families of complexity level two we obtain 2^3 families $\Sigma_{j,3}$, $j = 1, \ldots, 2^3$, of *complexity level three,* and so on. In this way all the symbolic sequences of cycles associated with the period adding structure are obtained.

To determine the analytic expressions of the BCB boundaries of the periodicity regions forming the period adding structure, consider first the basic cycles LR^{n_1} and RL^{n_1} belonging to the families $\Sigma_{1,1}$ and $\Sigma_{2,1}$ of complexity level one defined in (26). As shown in ([21]) and ([22]), the periodicity regions denoted $P_{LR^{n_1}}$ and $P_{RL^{n_1}}$ of map q are defined as

$$P_{LR^{n_1}} = \{p : \Psi_{1,1}(a_L, a_R, \mu_R, d, n_1) < \mu_L < \Phi_{1,1}(a_L, a_R, \mu_R, d, n_1)\}, \tag{30}$$

$$P_{RL^{n_1}} = \{p : \Psi_{1,1}(a_L, a_R, \mu_L, d, n_1) > \mu_R > \Phi_{1,1}(a_L, a_R, \mu_L, d, n_1)\}, \tag{31}$$

where

$$\Phi_{1,1}(a_L, a_R, \mu, d, n_1) = -\psi(a_R, n_1)\mu + \varphi(a_R, a_L, n_1)d,$$
$$\Psi_{1,1}(a_L, a_R, \mu, d, n_1) = -\left(a_L + \psi(a_R, n_1 - 1)\right)\mu + a_R\varphi(a_R, a_L, n_1)d,$$

with

$$\varphi(a, b, n) = \frac{1 - a^n b}{a^n}, \quad \psi(a, n) = \frac{1 - a^n}{(1 - a)a^n}.$$

The equations of the BCB boundaries are the boundaries of the existence regions, that is:

$$\mu_L = -\psi(a_R, n_1)\mu_R + \varphi(a_R, a_L, n_1)d, \quad \mu_L = -\left(a_L + \psi(a_R, n_1 - 1)\right)\mu_R + a_R\varphi(a_R, a_L, n_1)d,$$
$$\mu_R = -\psi(a_R, n_1)\mu_L + \varphi(a_R, a_L, n_1)d, \quad \mu_R = -\left(a_L + \psi(a_R, n_1 - 1)\right)\mu_L + a_R\varphi(a_R, a_L, n_1)d.$$

The formulas for the periodicity regions of the second and higher complexity levels are obtained by using the replacements (27) as explained in [22].

The expressions in (30) and (31), as well as the formulas for the other complexity levels, are valid for the map g given in (13) substituting

$$a_L = \frac{1 - \delta + ra}{1 + y^*}, \quad a_R = \frac{1 - \delta}{1 + y^*},$$
$$\mu_L = \frac{wc}{1 + y^*}, \quad \mu_R = \frac{w(b + c)}{1 + y^*}, \quad d = \frac{b}{a}.$$

For map g_1 given in (19), to describe the period adding structure associated with the branches $g_{LL}(x)$ and $g_{RL}(x)$, the following substitutions are to be performed in (30), (31):

$$a_L = \frac{(1 - \delta + ra)^2}{(1 + y_1)(1 + y_2)}, \quad \mu_L = \frac{(2 - \delta + ra + y_1)wc}{(1 + y_1)(1 + y_2)}, \quad d = \frac{b}{a},$$
$$a_R = \frac{(1 - \delta)(1 - \delta + ra)}{(1 + y_1)(1 + y_2)}, \quad \mu_R = \frac{(1 - \delta + ra)w(b + c) + (1 + y_1)wc}{(1 + y_1)(1 + y_2)},$$

where y_1, y_2 are given in (17). In Fig.5 this period adding structure structure issues from the point $p_1 = \xi_{LL}^{b/a} \cap \xi_{RL}^{b/a}$.

To get the boundaries of the periodicity regions related to the period adding structure of map g_1 (issuing from the point $p_2 = \xi_{RL}^{\overline{x_2}} \cap \xi_{RR}^{\overline{x_2}}$ in Fig.5) associated with the branches $g_{RL}(x)$ and $g_{RR}(x)$ the following substitutions are to be used:

$$a_L = \frac{(1 - \delta)(1 - \delta + ra)}{(1 + y_1)(1 + y_2)}, \quad \mu_L = \frac{(1 - \delta + ra)w(b + c) + (1 + y_1)wc}{(1 + y_1)(1 + y_2)},$$
$$a_R = \frac{(1 - \delta)^2}{(1 + y_1)(1 + y_2)}, \quad \mu_R = \frac{(2 - \delta + y_1)w(b + c)}{(1 + y_1)(1 + y_2)}, \quad d = \overline{x_2},$$

where $\overline{x_2}$ is defined in (19).